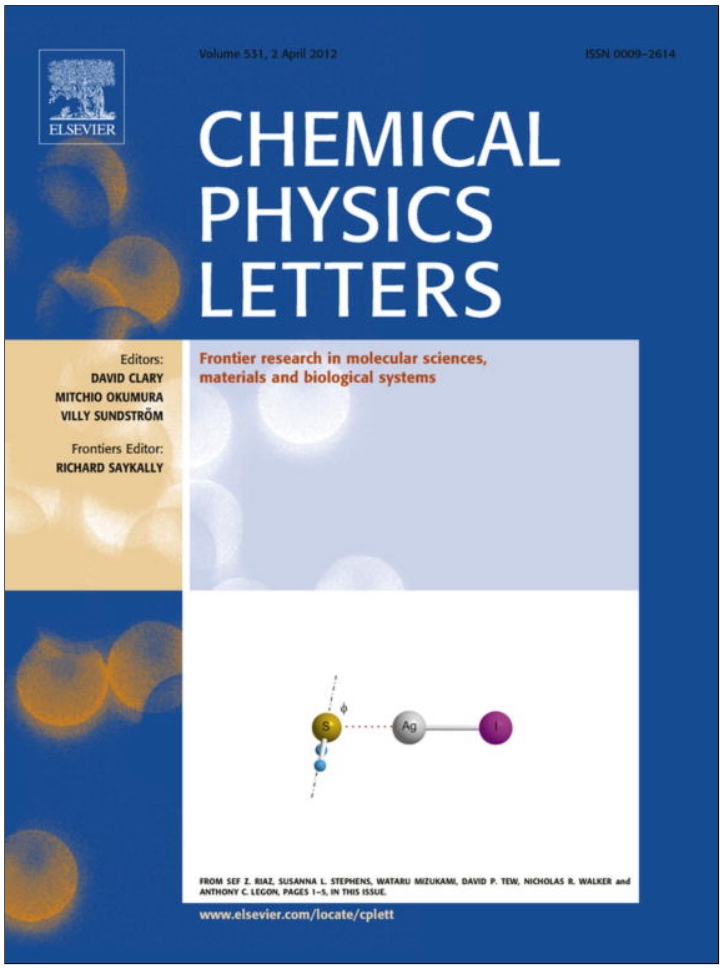

Chemical Physics Letters 531 (2012) 28–33

Contents lists available at SciVerse ScienceDirect

Chemical Physics Letters

journal homepage: www.elsevier.com/locate/cplett

A multiquantum dataset for vibrational excitation and dissociation in high-temperature O_2–O_2 collisions

M. Lino da Silva *, J. Loureiro, V. Guerra

Instituto de Plasmas e Fusão Nuclear, Laboratório Associado, Instituto Superior Técnico, Universidade Técnica de Lisboa, 1 Av. Rovisco Pais, 1049-001 Lisboa, Portugal

ARTICLE INFO

Article history:
Received 24 June 2011
In final form 30 January 2012
Available online 6 February 2012

ABSTRACT

The Forced Harmonic Oscillator (FHO) model is applied to the production of a multiquantum dataset of V–T and V–D rates for O_2–O_2 collisions, for T = 100–100 000 K. A simplified 1D O_2–O_2 intermolecular potential, accounting for long-range interactions, has been obtained through comparison of FHO and reference state-specific rates. A Morse potential with parameters $\alpha = 4\,\text{Å}^{-1}$ and E = 380 K provides the best fit between those. This potential has then been applied to the production of the overall multiquantum V–T and V–D rates, considering 47 vibrational levels. The resulting thermal dissociation rates agree remarkably well with experimental dissociation rates.

1. Introduction

The modeling of plasmas at high translational temperatures is a task which fosters challenges different from those involved in the modeling of lower temperature plasmas such as gas discharges. The accuracy of such high-temperature models is strongly dependent on the availability of a reliable dataset of heavy-impact vibration–translation (V–T) and vibration–dissociation (V–D) rates. It is known that simplified approaches such as the first-order perturbation theory (FOPT) fail at qualitatively and quantitatively describing such excitation processes. The FOPT approaches are known to over-predict single V–T rates at translational temperatures typically in excess of 2000 K. Moreover, they are also not capable of predicting multiquantum rates, therefore yielding lower rates of energy transfer towards molecular internal (vibrational) modes, as well as lower dissociation rates [1,2]. Although these effects may coincidentally balance out, it is clear that efforts should be steered away from such simplified models.

With this knowledge at hand, several research teams have put an effort at providing more accurate heavy-impact datasets. High-fidelity approaches for the modeling of V–T and V–V transitions in molecular collisions have firstly been introduced by Billing and his co-workers, which developed and applied semi-classical collisional methods for the description of collisional processes in nitrogen, oxygen and hydrogen [3–5]. These methods where then extended for other collisional pairs (H_2–H_2, N_2–CO, N_2–N_2) in collaboration with and by the Bari group [6–10].

Approaches involving a larger number of higher lying vibrational states, and providing reliable multiquantum rates for the overall manifold of molecular vibrational levels, have been introduced by Esposito and Capitelli [11,12]. These authors considered a Quasi-Classical Trajectory (QCT) model for the calculation of V–T and V–D collisions for atom–diatom N_2 collisions, considering a Potential Energy Surface (PES) provided by Laganà [13]. More recently, Jaffe has utilized a similar approach [14], relying on the PES proposed by Wang [15] for this same collision system. For diatom–diatom collisions, our group has recently applied the Forced Harmonic Oscillator (FHO) theory to produce a complete dataset of reactions for N_2–N_2 collisions [16]. More recently, a semiclassical method has been applied by Kurnosov et al. [17], who proposed rates for the same collision system, as well as for N_2–CO.

1.1. Previous studies on the vibrational relaxation of oxygen

For O–O_2 collisions, a dataset based on the QCT approach has been proposed by Esposito et al. [18,19], based on a PES calculated by Varandas and Pais [20]. This Letter encompasses all the possible multiquantum transitions for the overall manifold of vibrational levels of O_2, yielding a complete dataset applicable as high as 10 000 K.

For diatom–diatom collisions of O_2, the previous works available in the literature have been mainly focused on the modeling of chemical processes in Earth's upper atmosphere, and they are mainly related to the production of Ozone (see Refs. [21,22], which consider the intermolecular potential of Ref. [23]). Such works often limit themselves to the calculation of V–V exchange processes at high vibrational levels ($v \geqslant 8$) and low temperatures ($T \leqslant 500\,\text{K}$), with the exception of a more recent work by Coletti and Billing [5], which propose a larger dataset of V–T and V–V rates in the vibrational levels range ($1 \leqslant v \leqslant 29$), and in the temperature range ($50\,\text{K} \leqslant T \leqslant 1000\,\text{K}$). To obtain such a dataset, an updated version of the intermolecular potential proposed in Ref. [24],

* Corresponding author. Fax: +351 21 846 44 55.
E-mail addresses: mlinodasilva@mail.ist.utl.pt, mlinodasilva@ist.utl.pt (M. Lino da Silva).

0009-2614/$ - see front matter © 2012 Elsevier B.V. All rights reserved.
doi:10.1016/j.cplett.2012.01.074

accounting for the effects of molecular rotation, is considered and the obtained rates are compared to those obtained considering an older potential (Ref. [4]).

Although these datasets exhibit a high-enough degree of accuracy for applications such as atmospheric chemistry or gas discharges, they are limited to fairly low-temperature ranges. The datasets are produced for $T \leqslant 1000\,K$ and further they do not provide all the possible multiquantum rates over the overall manifold of vibrational levels up to dissociation. In order to fill such a gap, we propose to complement these works with a novel dataset for vibrational excitation and dissociation by O_2–O_2 collisions, based on the FHO approach previously considered for the N_2 dataset developed by our group.

It is nevertheless evident that a method resorting to a 1D Morse potential cannot produce a manifold of vibrational transitions as accurate as a method resorting to a full 3D potential, obtained through more detailed quantum chemistry approaches. However, the objective of this Letter is not to provide a 'reference' set of state-specific vibrational transition data, but instead to provide a bridging method capable of providing a complete dataset of rates for O_2–O_2 vibrational transitions, which is at worst physically consistent and at best high-temperature accurate and reasonable at low-temperatures.

A dataset including all the possible multiquantum V–T transitions for O_2–O_2 collisions is therefore proposed in this Letter. A thorough validation of such a dataset is difficult, as no experimentally-determined or calculated multiquantum rates are currently available for comparison (to the authors knowledge). Therefore, the multiquantum rates obtained through the FHO model have to be indirectly validated. This is achieved through the comparison of the predicted thermal dissociation rate against reference experimental dissociation rates, as a correct behavior of dissociation processes in equilibrium conditions is evidence that the predicted state-specific multiquantum rates are at least consistent.

2. Methods

Our research group has been favoring the more general semiclassic, analytical FHO approach, from which the well known FOPT approach is derived [25–27]. Such an approach presents the advantage of being (essentially) an analytical approach, which is capable of yielding results comparable to non-analytic semiclassical and quantum approaches, without the associated model complexity and computational burdens. As such, this approach has gained a renewed interest following the extensions and generalizations[1] proposed by Adamovich and Macheret [28–31]. Lastly, considering a proper tailoring of the numerical calculation of the FHO transition probabilities, and the proper selection of an overall manifold of vibrational levels, Lino da Silva et al. have shown that the FHO theory can yield detailed and reliable V–T and V–D non-reactive rates for diatom–diatom collisions, over a very extended temperature range [1,16,32].

The selection of an adequate intermolecular potential is of paramount importance for the calculation of adequate transition probabilities and rates. As a result of the extensions of the FHO theory proposed by Adamovich and Macheret, one may either consider a more restricted 1D description of the collisional process [29], or a more general 3D description [31] without the inclusion of any steric factors. Still this more general analytical description comes at a cost, as it can only account for fully repulsive intermolecular potentials. On the other hand, the 1D description can accommodate a more detailed Morse intermolecular potential, accounting for both short-range repulsive forces as well as any long range attractive forces.

In our works, we have chosen to restrict ourselves to a 1D description, with the generalization to 3D collisions through the application of steric factors. Indeed it has been found that the application of steric factors, for the generalization of 1D head-on collisions to 3D trajectories, yields reasonably good reaction rates [1,16]. More importantly, this allows us to consider a more complex Morse intermolecular potential. While full 3D models can yield very accurate results at translational temperatures as low as 1000 K for interactions which are essentially repulsive (such as for example the N_2–N_2 pair, with an attractive potential as low as 200 K [33,17]), they cannot yield accurate low-temperature state-resolved rates for collisions where the attractive part of the intermolecular potential is non-negligible. Such is the case for O_2–O_2 collisions as it is shown in this Letter.

2.1. Calculation of the vibrational levels and associated energies for O_2

An important improvement which we include in our model is the selection of an accurate manifold of vibrational levels. As we discuss in a previous work [32], the traditional approach of considering popular polynomial expansions for the determination of the number of vibrational levels and their associated energies is inherently flawed, as such polynomial expansions are extrapolated well beyond their range of validity. Instead, we chose either to select an accurate intramolecular potential curve from the literature (if available), or to rebuild one using an extrapolated RKR method [32]. Then, solving the radial Schrödinger equation over this potential, achieved through a Discrete Fourier Grid Transform method, yields the adequate manifold of vibrational level energies. This method typically returns a number of vibrational levels which is significantly different from those obtained through a polynomial expansion (61 instead of 46 for the ground state of N_2 [32]). The input of these differing manifolds of vibrational levels in state-specific dissociation–recombination models returns thermal dissociation rates with differences of several orders of magnitude [2]. Significant differences are also predicted for the time-dependent populations of excited species [32].

In the case of the ground state of O_2, we have considered the spectroscopic constants from Ref. [34] to rebuild the potential curve through an extrapolated RKR method. Solving the radial

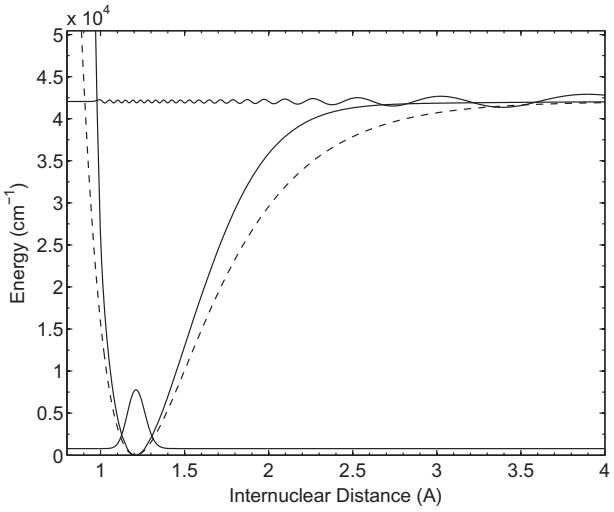

Figure 1. Reconstructed potential curve for the ground state of O_2, with the scaled wavefunction of the first ($v = 0$) and last ($v = 46$) vibrational levels shown. The corresponding Morse potential (– –) is also represented.

[1] These account for the anharmonicity of intramolecular potential curves; enforcing detailed balance through the symmetrization of the collision energies; etc.

Schrödinger equation returned a set of 47 bound vibrational levels, as pictured in Figure 1.

The reconstructed energies can be fitted to a traditional polynomial expansion:

$$E(v) = 1560\left(v+\frac{1}{2}\right) + 3.7912\times10^{-3}\left(v+\frac{1}{2}\right)^2 - 2.397\left(v+\frac{1}{2}\right)^3 + 0.23527\left(v+\frac{1}{2}\right)^4 - 0.012185\left(v+\frac{1}{2}\right)^5 + 3.445\times10^{-4}\left(v+\frac{1}{2}\right)^6 - 5.0792\times10^{-6}\left(v+\frac{1}{2}\right)^7 + 3.0408\times10^{-8}\left(v+\frac{1}{2}\right)^8 \quad (1)$$

We verify that the reconstructed potential differs significantly from the Morse potential which can be obtained by considering the same spectroscopic constants (Ref. [34]). Unsurprisingly, solving the Schrödinger equation over this potential yields significantly different energy levels over the whole vibrational range, with a predicted maximum vibrational level of 62 instead of 46.

2.2. Intermolecular potential

As previously mentioned, once a reliable theoretical model is selected, and the proper manifold of vibrational levels is obtained, all that remains is the definition of an adequate intermolecular potential. From the previous works of Adamovich, it has been found that a fully repulsive potential with the parameter $\alpha = 4\,\text{Å}^{-1}$ yields reliable O_2–O_2 V–T rates in the high-temperature limit (>1000 K) [1]. However, in the low-temperature limit, the obtained rates were several orders of magnitude below other rates published by Billing [4]. Our approach consisted in estimating the best Morse intermolecular potential which would be capable of reproducing these higher-fidelity semi-classical results from Billing. Different Morse intermolecular potentials, $V(r) \sim E_m(1-\exp(-\alpha r))^2$, have been iterated with a fixed repulsive parameter $\alpha = 4\,\text{Å}^{-1}$, and a variable potential well E, accounting for long-range attractive interactions. The best fit against Billing's rates has been obtained for $E = 380$ K, as shown in Figure 2. The corresponding rates of the FHO model, for a fully repulsive potential, are also shown. As we can attest from the numerical results, the effects of the attractive part of the potential are more apparent at lower temperatures, becoming essentially negligible above 5000 K.

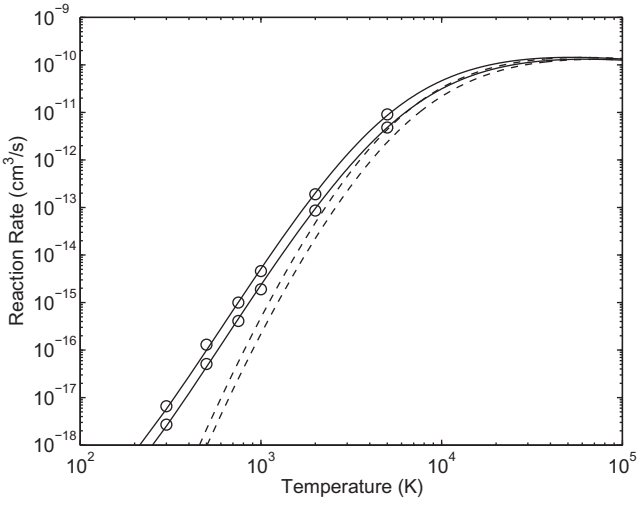

Figure 2. Single-quantum V–T rates for $1 \to 0$ and $2 \to 1$ transitions (bottom to top). –, FHO model ($E = 380$ K); – –, FHO model (repulsive potential); ○, calculations of Ref. [5].

2.3. Model validation in the low-temperature range

Some further comparisons have also been carried against the more recent semi-classical calculations from Coletti and Billing [5], for the reaction pair:

$$O_2(v) + O_2(0) \to O_2(v-1) + O_2(1) \quad \text{(V–V)} \quad (2)$$

$$O_2(v) + O_2(0) \to O_2(v-1) + O_2(0) \quad \text{(V–T)} \quad (3)$$

It is of particular interest to compare the FHO model against other resonant and near-resonant V–V rates, as it is known that one of the small flaws of the FHO model is precisely its underestimation of such rates at low-temperatures, given that the model intrinsically treats V–V rates as a product of single-quantum V–T rates [28,1]. As we can attest in the topmost part of Figure 3, the FHO rate under-predicts the resonant exchange rate (for $v = 1$) at $T = 100$ K, followed by a decrease of the difference between the FHO rate and the rate of Coletti and Billing, as we move to larger quanta, farther from resonance. As expected, this effect no longer subsides at higher temperatures ($T = 1000$ K) where the two rates are almost equivalent, the FHO rate being slightly larger (less than one order of magnitude). These differences can be mitigated by reverting to an FOPT approach for such type of rates [28]. In the case of near-resonant V–V rates, it is very important to properly quantify the energy gaps between the different vibrational levels.

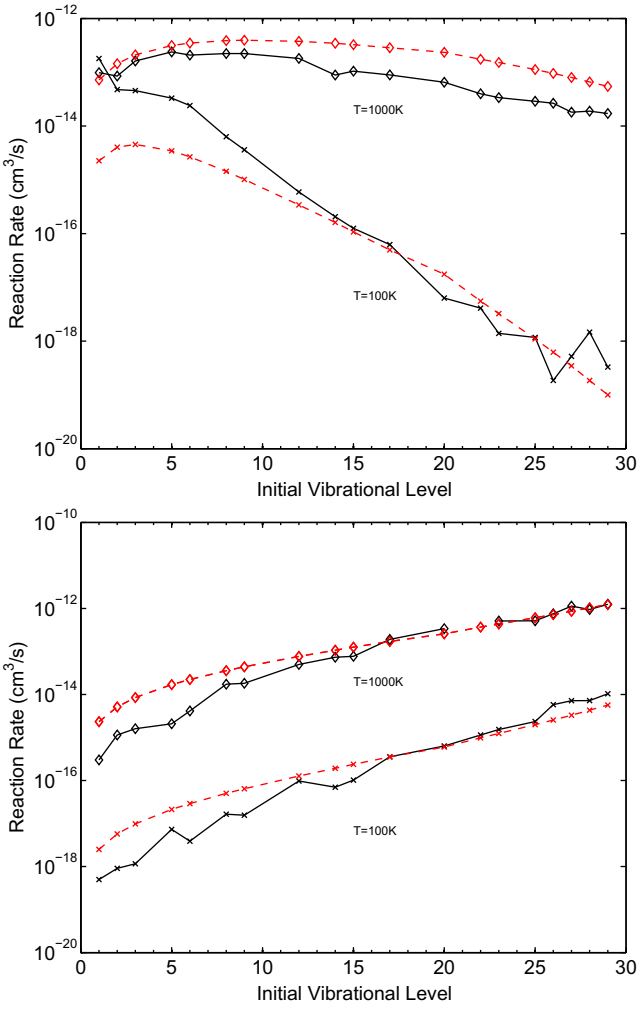

Figure 3. Single-quantum V–V (top figure) and V–T (bottom figure) rates for the reactions of Eqs. (2) and (3). – –, FHO model; –, calculations of Ref. [5].

Here we consider the more accurate extrapolated RKR method for the calculation of these level energies, whereas Coletti and Billing consider a much more simplistic Morse potential (Figure 1). In view of the different potentials taken into consideration, it is expected to have increasing differences in the level energies predicted by the RKR method and those predicted by the Morse approximation. However, the lower vibrational levels should be essentially equivalent, and the differences in the predicted rates are most certainly a result of the different theoretical approaches that are utilized in the respective works. As for the non-resonant FHO V–T rates (bottommost part of Figure 3), they show an excellent agreement with those of Coletti and Billing for the relaxation of the excited v-levels ($v > 10$), whereas the agreement is less satisfactory for lower v-states. Furthermore, the FHO rates present the advantage of being more homogeneous than those obtained by these methods, which rely on the sampling of trajectories.

These different validations show that the FHO model can be utilized with confidence for the production of multiquantum V–T rates, considering an average Morse intermolecular potential with $\alpha = 4\ \text{Å}^{-1}$ and $E = 380$ K. Figure 4 shows a comparison between our simplified isotropic potential, and the angle-averaged potential of Coletti and Billing. We verify that the averaged potential well is unrealistically low (about 110 K), as compared to our semi-empirical potential well of 380 K, or even the potential well of essentially repulsive collision pairs such as N_2–N_2 [33]. Interestingly enough, if we replace the repulsive potential parameter α recommended by Coletti and Billing ($3.436\ \text{Å}^{-1}$) by the one recommended by Adamovich ($4\ \text{Å}^{-1}$) [33], we obtain a potential well very close to ours (about 440 K).

In the next part of the Letter we will discuss the overall dataset of multiquantum V–T and V–D reactions that has been produced using this model.

3. Results

As discussed here for O_2 and in previous papers [1,2,16] for N_2, the FHO approach is essentially semi-analytic, only mandating carefully tailored methods for avoiding overflows and underflows (as the result of factorization operations introduced by the theory [1]). This comes as an advantage, as a complete set of V–T and V–D rates can be produced without the need to conduct extensive trajectories calculations such as with trajectory sampling methods. Therefore, one may easily obtain a set of thousands of noiseless rates within a week or two of calculations with a standard PC.

As for our previous work with N_2–N_2 collisions, we consider that pure V–V exchange processes can be neglected (a reasonable assumption for roughly $T \geqslant 10\,000$ K [28]), and we mainly perform a scaling of the FHO transition probability such that:

$$P(i_1, \text{all} \rightarrow f_1, \text{all}, \varepsilon, \rho) = P(i_1 \rightarrow f_1, \varepsilon) \tag{4}$$

where ε and ρ are related to the two-state FOPT transition probabilities, with $\varepsilon = P_{\text{FOPT}}(1 \rightarrow 0)$ and $\rho = [4P_{\text{FOPT}}(1, 0 \rightarrow 0, 1)]^{1/2}$.

State-specific V–D dissociation rates are calculated according to:

$$P(i \rightarrow, \varepsilon) = P(i \rightarrow v_{qbound}, \varepsilon) \cdot P_{decay} \tag{5}$$

with $P_{\text{decay}} \sim 1$, and $v_{\text{qbound}} = v(>46)$.

Considering such approximations, we finally obtain a dataset of $(46+1)^2$ V–T rates and 47 V–D rates for a temperature range $T = [100\text{–}1\,00\,000$ K] by steps of 100 K. A sample of the overall multiquantum V–T rates at $T = 10{,}000$ K is presented in Figure 5. The V–D dissociation rates for the initial vibrational levels $v = 0$, $v = 10$, $v = 20$ and $v = 30$ are presented for the temperature range $T = 1000$ K–$1\,00\,000$ K in Figure 6.

The V–D rates have been validated following the approach outlined in [16]. The corresponding thermal dissociation rates are obtained according to the equation:

$$\begin{aligned} K_d(T) &= \sum_v K_d(v, T) \times \frac{N_v(T)}{N} \\ &= \sum_v K_d(v, T) \times \frac{Q_v(T)}{\sum_v Q_v(T)} \end{aligned} \tag{6}$$

and are then compared to the several thermal dissociation rates proposed in popular chemical datasets from the literature, which mostly derive from shock-tube experiments carried at high temperatures. The different rates are presented in Table 1. These rates have been merged together in order to provide the lower and upper bounds against which our thermal FHO dissociation rate is to be compared. Such a comparison is presented in Figure 7.

As it can attested by such a comparison, our FHO model provides high-temperature dissociation rates in excellent agreement with those derived from popular chemical datasets (which themselves derive from experimental rates). Even in the low-

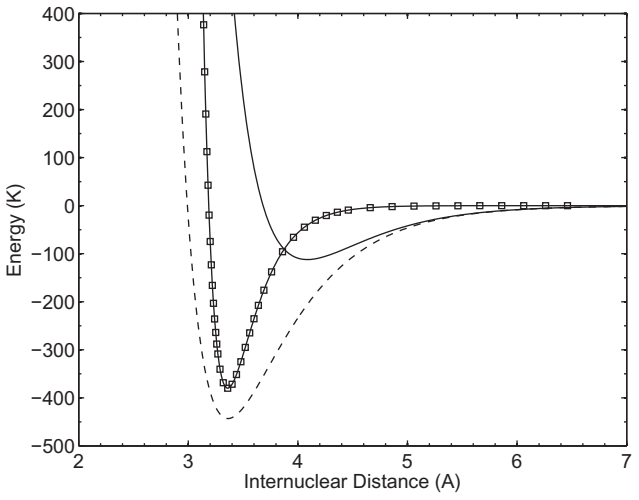

Figure 4. Angle-averaged potential energy for O_2–O_2 interactions, at fixed equilibrium internuclear distances, and with repulsive parameters $\alpha = 3.436\ \text{Å}^{-1}$ (–) and $\alpha = 4\ \text{Å}^{-1}$ (–), from the analytic expression of Ref. [5] (– –). The isotropic 1D Morse intermolecular potential proposed in this Letter is also presented for comparison (–□–).

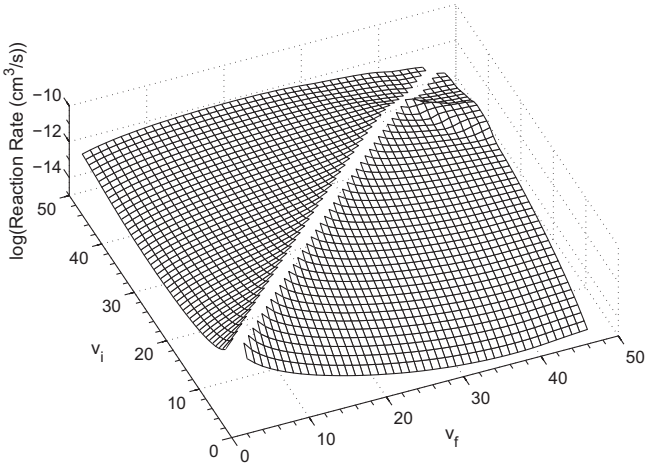

Figure 5. V–T reaction rates at 10 000 K. v_i and v_f denote the initial and final vth level in the transition.

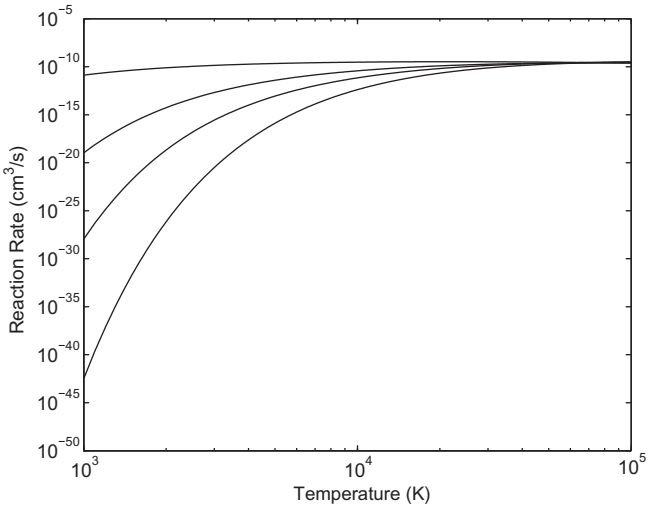

Figure 6. V–D reaction rates for the initial vibrational levels $v = 0$, $v = 10$, $v = 20$ and $v = 30$ (bottom to top).

Table 1
Rates for reaction $O_2 + O_2 \rightarrow O + O + O_2$ (cm^3/s).

Dunn & Kang [35]	$5.38 \times 10^{-5} T^{-1.0} \exp(-59500/T)$
Moss [36]	$5.39 \times 10^{-5} T^{-1.0} \exp(-59400/T)$
Gardiner [37]	$2.72 \times 10^{-5} T^{-1.0} \exp(-59380/T)$
Park [38,39]	$3.32 \times 10^{-3} T^{-1.5} \exp(-59500/T)$
Brenner [41]	$4.58 \times 10^{-5} T^{-1.0} \exp(-59500/T)$
Shatalov [40]	$3.91 \times 10^{-5} T^{-0.645} \exp(-59874/T)$

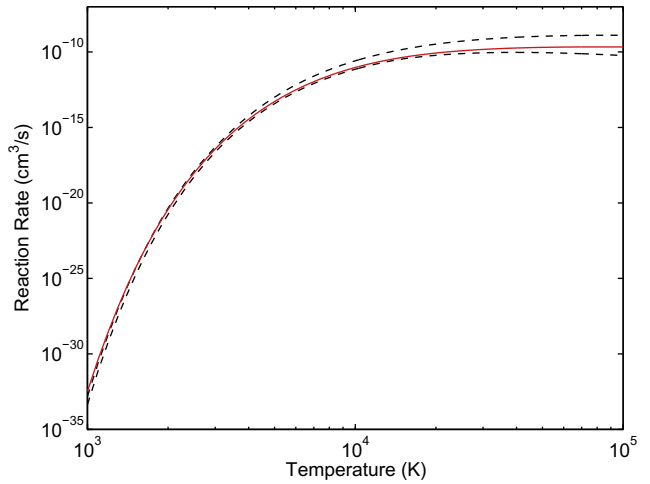

Figure 7. Comparison of the O_2–O_2 thermal dissociation rate obtained from the FHO model (–) with the upper and lower bounds of the experimentally determined dissociation rates of Table 1 (– –).

temperature limit (around 1000 K), the FHO dissociation rate follows very closely the sharp decrease in the experimental dissociation rates. In the low-temperature limit (1000 K), the FHO dissociation rate is only a factor of 1.5 above the upper bound of the experimental rates, for a value around 5×10^{-31} cm^3/s, which anyway is essentially negligible.

In short, the different validations presented in this Letter show that the proposed FHO dataset provides detailed and reliable V–T and V–D rates over a very large temperature range.

4. Conclusions

In this Letter, we have have proposed a complete multiquantum dataset for O_2–O_2 V–T and V–D collisional transitions, which complements the other available datasets for these kind of reactions, recently proposed by ourselves and other authors (and referenced herein). These rates, produced in 100 K intervals in the temperature range [100–1 00 000 K], for the overall possible multiquantum transitions can be made available to the community upon request.

In the low-temperature limit, our proposed rates have been compared to high fidelity rates from previous works mainly focused in the chemistry of the higher atmosphere. It has been found that our FHO rates reproduce quite effectively these previous rates, except for resonant and near-resonant rates – a known weakness of the FHO approach – at temperatures where translation–vibration energy transfer processes are limited. In the high-temperature limit, our produced V–D dissociation rates have shown an excellent agreement with thermal dissociation rates issued from the literature. More importantly, the overall manifold of possible multiquantum V–T and V–D rates for O_2–O_2 collisions has been made available for the first time, through the application of our approach to the FHO model. In short, this Letter provides a valuable contribution towards the improvement of the different state-resolved kinetic models considered in a large array of applications (from low-temperature gas-discharge and atmospheric chemistry experiments, to high-temperature combustion and shock-tube experiments).

For example, the introduction of this new dataset should in principle suffice for allowing the design of sounder and more accurate kinetic models for the simulation of high-temperature plasmas. Firstly, collisional rates with different colliding partners (such as for example O_2–N or N_2–O_2) could be scaled from existing rates (in this case O_2–O and N_2–N_2), by simply considering a corrective factor accounting for the differences in the reduced masses. Although this approach might appear crude as compared with a more detailed approach of building a complete dataset using a QCT or FHO method, it is considerably less time-consuming and should still provide reasonably detailed and reliable results. Secondly, datasets for the very important Zeldovitch reactions of NO with atomic N and O are also available in the literature [42,43], and should sufice for the accounting of interacting NO molecules within the plasma. As the molar fractions of such a species is typically low, non-reactive impact reactions with NO could in principle be neglected.

The production of such complete dataset of heavy-impact reactions, coupled to the several electron-impact datasets already proposed in the literature, would yield a detailed and reliable state-to-state model which would be applicable to a large array of high or low-temperature plasmas, possibly yielding a more accurate description of the elementary processes therein.

References

[1] M. Lino da Silva, V. Guerra, J. Loureiro, J. Thermophys. Heat Transf. 21 (1) (2007) 40.
[2] M. Lino da Silva, V. Guerra, J. Loureiro, Plasma Sourc. Sci. Technol. 18 (2009) 034023.
[3] G.D. Billing, Vibration–vibration and vibration–translation energy transfer including multiquantum transitions in atom–diatom and diatom–diatom collisions, in: M. Capitelli (Ed.), Topics in Current Physics: Nonequilibrium Vibrational Kinetics, Springer-Verlag, Berlin, Heidelberg, 1986, p. 85.
[4] G.D. Billing, R.E. Kolesnick, Chem. Phys. Lett. 200 (4) (1992) 382.
[5] C. Coletti, G.D. Billing, Chem. Phys. Lett. 356 (1) (2002) 14.
[6] M. Cacciatore, G.D. Billing, J. Phys. Chem. 96 (1) (1992) 217.
[7] A. Kurnosov, M. Cacciatore, G.D. Billing, J. Phys. Chem. A 107 (14) (2003) 2403.
[8] M. Cacciatore, A. Kurnosov, A. Napartovich, S. Shnyrev, J. Phys. B: At. Mol. Opt. Phys. 37 (16) (2004) 3379.
[9] M. Cacciatore, A. Kurnosov, A. Napartovich, J. Chem. Phys. 123 (2005) 1743151.
[10] A. Kurnosov, A. Napartovich, S. Shnyrev, M. Cacciatore, J. Phys. Chem. A 111 (30) (2007) 7057.

[11] F. Esposito, M. Capitelli, C. Gorse, Chem. Phys. 257 (2–3) (2000) 193.
[12] F. Esposito, I. Armenise, M. Capitelli, Chem. Phys. 331 (1) (2006) 1.
[13] A. Lagana, E. Garcia, J. Phys. Chem. 98 (1994) 502.
[14] R. Jaffe, D. Schwenke, G. Chaban, W. Huo, AIAA Paper AIAA-2008-1208, 46th AIAA Aerospace Sciences Meeting and Exhibit, Orlando, FL, 7–10 January, 2008.
[15] D. Wang D, W.M. Huo, C.E. Dateo, D.W. Shwenke, J.R. Stallcop, J. Chem. Phys. 120 (13) (2004) 6041.
[16] M. Lino da Silva, V. Guerra, J. Loureiro, J. Thermophys. Heat Transf. 21 (2) (2007) 303.
[17] A.K. Kurnosov, A.P. Napartovich, S.L. Shnyrev, M. Cacciatore, Plasma Sourc. Sci. Technol. 19 (4) (2010) 045015.
[18] F. Esposito, M. Capitelli, Chem. Phys. Lett. 443 (4–6) (2007) 222.
[19] F. Esposito, M. Capitelli, Chem. Phys. 351 (1–3) (2008) 91.
[20] A.J.C. Varandas, A.A.C.C. Pais, Mol. Phys. 65 (4) (1988) 843.
[21] N. Balakrishnan, A. Dalgarno, G.D. Billing, Chem. Phys. Lett. 288 (5–6) (1998) 657.
[22] J. Campos-Martinez, E. Carmona-Novillo, J. Echave, M.I. Hernandez, R. Hernandez-Lamoneda, J. Palma, Chem. Phys. Lett. 289 (1–2) (1998) 150.
[23] A.J.C. Varandas, W. Wang, Chem. Phys. 215 (2) (1997) 167.
[24] V. Aquilanti, D. Ascenzi, M. Bartolomei, D. Cappelletti, S. Cavalli, M. de Castro Vitores, F. Pirani, J. Am. Chem. Soc. 121 (46) (1999) 10794.
[25] E.H. Kerner, Can. J. Phys. 36 (3) (1958) 371.
[26] C.E. Treanor, J. Chem. Phys. 43 (2) (1965) 532.
[27] A. Zelechow, D. Rapp, T.E. Sharp, J. Chem. Phys. 49 (1) (1968) 286.
[28] I.V. Adamovich, S.O. Macheret, J.W. Rich, C.E. Treanor, AIAA J. 33 (6) (1995) 1064.
[29] I.V. Adamovich, J.W. Rich, J. Chem. Phys. 109 (18) (1998) 7711.
[30] S.O. Macheret, I.V. Adamovich, J. Chem. Phys. 113 (17) (2000) 7351.
[31] I.V. Adamovich, AIAA J. 39 (10) (2001) 1916.
[32] M. Lino da Silva, V. Guerra, J. Loureiro, P.A. Sá, Chem. Phys. 348 (1–3) (2008) 187.
[33] I.V. Adamovich, S.O. Macheret, J.W. Rich, C.E. Treanor, J. Thermophys. Heat Transf. 12 (1) (1998) 57.
[34] D.L. Albritton, A.L. Schmeltekopf, R.N. Zare, Unpublished results reported in C. Laux, Optical Diagnostics and Radiative Emission of Air Plasmas, Ph.D. Thesis, Stanford University, 1993.
[35] M.G. Dunn, S.W. Kang, Theoretical and Experimental Studies of Re-Entry Plasmas, NASA CR-2232, April 1973.
[36] J.L. Shinn, J.N. Moss, A.L. Simmonds, AIAA Paper 82-0842, 3rd Joint Thermophysics, Fluids, Plasma and Heat Transfer Conference, St. Louis, MO, 7–11 June, 1982.
[37] W.C. Gardiner, Combustion Theory, Springer Verlag, Berlin, 1984.
[38] C. Park, AIAA Paper 89-1740, 24th Thermophysics Conference, Buffalo, NY, 12–14 June, 1989.
[39] C. Park, R.L. Jaffe, H. Partridge, J. Thermophys. Heat Transf. 15 (1) (2001) 76.
[40] O.P. Shatalov, Recommended Data on Rate Constants of Physical and Chemical Processes in N–O Atoms System, Moscow State University – Russia, Institut of Mechanics AVOGADRO Center.
[41] Uncited reference in William J., étude des Processus Physico-Chimiques Dans les écoulements Détendus à Haute Enthalpie: Application à la Soufflerie à Arc F4, Ph.D. Thesis (in French), Université de Provence, France, 1999.
[42] D. Bose, G.V. Candler, J. Thermophys. Heat Transf. 10 (1) (1996) 148.
[43] D. Bose, G.V. Candler, J. Chem. Phys. 104 (8) (1996) 2825.